2 Significance of Ductal Region in Anaplastic Pancreatic Cancer. K. Miura, K. Kimura, R. Amano, S. Yamazoe, G. Ohira, K. Nishio, M. Shibutani, K. Sakurai, H. Nagahara, T. Toyokawa, N. Kubo, H. Tanaka, K. Muguruma, H.Otani, M. Yashiro, K. Maeda, M. Ohira, K. Hirakawa.
APA/JPS 45th Anniversary Meeting
November 5-8, 2014 Hawaii, Meeting Proceeding p29, P1-51.

3 Importance of the Invasive Distance in Invasive IPMN as a Prognostic Factor. K. Kimura, R. Amano, S. Yamazoe, K. Miura, G. Ohira, K. Nishio, M. Shibutani, K. Sakurai, H. Nagahara, T. Toyokawa, N. Kubo, H. Tanaka, K. Muguruma, H. Otani, K. Maeda, M. Ohira, K. Hirakawa.
APA/JPS 45th Anniversary Meeting
November 5-8, 2014 Hawaii, Meeting Proceeding p40, P2-80

4 Persisting Elevation of Postoperative CRP Predicts Outcome of Patients with Curative Distal Pancreatectomy for Pancreatic Cancer. S.Yamazoe, R.Amano K.Kimura K.Hirata K.Miura K.Hirakawa.
APA/JPS 45th Anniversary Meeting
November 5-8, 2014 Hawaii, Meeting Proceeding p47, P3-46.

H. 知的財産権の出願・登録状況（予定を含む。）
なし。

様式第１９

学　会　等　発　表　実　績

委託業務題目「膵管内乳頭粘液腫瘍患者における超早期膵癌捕捉技術の開発」
機関名　公立大学法人　大阪市立大学医学研究科

１．学会等における口頭・ポスター発表

発表した成果（発表題目、口頭・ポスター発表の別）	発表者氏名	発表した場所（学会等名）	発表した時期	国内・外の別
Significance of Ductal Region in Anaplastic Pancreatic Cancer.（ポスター）	K. Miura, K. Kimura, R. Amano, S. Yamazoe, G. Ohira, K. Nishio, M. Shibutani, K. Sakurai, H. Nagahara, T. Toyokawa, N. Kubo, H. Tanaka, K. Muguruma, H. Otani, M. Yashiro, K. Maeda, M. Ohira, K. Hirakawa.	APA/JPS 45th Anniversary Meeting	November 5-8, 2014	国外
Importance of the Invasive Distance in Invasive IPMN as a Prognostic Factor.（ポスター）	K. Kimura, R. Amano, S. Yamazoe, K. Miura, G. Ohira, K. Nishio, M. Shibutani, K. Sakurai, H. Nagahara, T. Toyokawa, N. Kubo, H. Tanaka, K. Muguruma, H. Otani, K. Maeda, M. Ohira, K. Hirakawa.	APA/JPS 45th Anniversary Meeting	November 5-8, 2014	国外
Persisting Elevation of Postoperative CRP Predicts Outcome of Patients with Curative Distal Pancreatectomy for Pancreatic Cancer.（ポスター）	S. Yamazoe, R. Amano K. Kimura K. Hirata K. Miura K. Hirakawa.	APA/JPS 45th Anniversary Meeting	November 5-8, 2014	国外
CpG islands and genomic regions with basal low-level methylation to aberrant DNA methylation induction（口演）	Yamashita S, Nanjo S, Rehnberg E, Ando T, Maekita T, Ichinose M, Sugiyama T, Ushijima T	第8回日本エピジェネティクス研究会年会	2014年5月26日	国内
遺伝子点突然変異のターゲットシークエンシングによる高感度解析法の開発とGeneticな発がんの素地の解析（口演）	山下 聡, 岸野貴賢, 永野玲子, 牛島俊和	第29回発癌病理研究会	2014年9月3日	国内
High-Sensitivity Analysis of Aberrant DNA Methylation by Targeted Deep Sequencing using a Benchtop Sequencer.（口演）	Yamashita S, Kishino T, Nagano R, Ushijima T	第73回日本癌学会学術総会	2014年9月25日	国内
エクソソーム中のマイクロRNA発現解析は脂肪肝診断に有用である.（口演）	藤井英樹 豊田秀徳 村上善基	第18回日本肝臓学会大会	2014年10月23日	国内
miRNAによる肝線維化の抑制（口演）	村上善基	第41回日本毒性学会学術集会	2014年7月3日	国内
京都大学病院がんセンターキャンサーバイオバンクプロジェクト（口演）	金井雅史、古川恵子、松本繁巳、米澤淳、志賀修一、鶴山竜昭、黒田知宏、松原和夫、千葉勉、武藤学	第12回日本臨床腫瘍学会学術集会	2014年7月17日	国内

２．学会誌・雑誌等における論文掲載

掲載した論文（発表題目）	発表者氏名	発表した場所 （学会誌・雑誌等名）	発表した時期	国内・外の別
Positioning of 18F-fluorodeoxyglucose-positron emission tomography imaging in the management algorithm of hepatocellular carcinoma.	Kawamura E, Shiomi S, Kotani K, Kawabe J, Hagihara A, Fujii H, Uchida-Kobayashi S, Iwai S, Morikawa H, Enomoto M, Murakami Y, Tamori A, Kawada N	J Gastroenterol Hepatol	2014 Sep;29(9):1722-7.	国外
A phase I study of the combination chemotherapy of sorafenib and transcatheter arterial infusion with cisplatin for advanced hepatocellular carcinoma.	Hagihara A, Ikeda M, Ueno H, Morizane C, Kondo S, Nakachi K, Mitsunaga S, Shimizu S, Kojima Y, Suzuki E, Katayama K, Imanaka K, Tamai C, Inaba Y, Sato Y, Kato M, Okusaka T	Cancer Sci	2014 Mar;105(3):354-8	国外
Cytoglobin is expressed in hepatic stellate cells, but not in myofibroblasts, in normal and fibrotic human liver.	Motoyama H, Komiya T, Thuy le TT, Tamori A, Enomoto M, Morikawa H, Iwai S, Uchida-Kobayashi S, Fujii H, Hagihara A, Kawamura E, Murakami Y, Yoshizato K, Kawada N.	Lab Invest	2014 Feb;94(2):192-207.	国外
Relationship between inosine triphosphate genotype and outcome of extended therapy in hepatitis C virus patients with a late viral response to pegylated-interferon and ribavirin.	Hai H, Tamori A, Enomoto M, Morikawa H, Uchida-Kobayashi S, Fujii H, Hagihara A, Kawamura E, Thuy le TT, Tanaka Y, Kawada N.	J Gastroenterol Hepatol.	2014 Jan;29(1):201-7.	国外
A complete response induced by 21-day sorafenib therapy in a patient with advanced hepatocellular carcinoma	Hagihara A, Teranishi Y, Kawamura E, Fujii H, Iwai S, Morikawa H, Enomoto M, Tamori A, Kawada N.	Intern Med	2013;52(14):1589-92	国外
Identification of 27 5' CpG islands aberrantly methylated and 13 genes silenced in human pancreatic cancers	Hagihara A, Miyamoto K, Furuta J, Hiraoka N, Wakazono K, Seki S, Fukushima S, Tsao MS, Sugimura T, Ushijima T.	Oncogene	2004 Nov 11;23(53):8705-10.	国外
ZNF695 methylation predicts a response of esophageal squamous cell carcinoma to definitive chemoradiotherapy.	Takahashi T, Yamashita S, Matsuda Y, Kishino T, Nakajima T, Kushima R, Kato K, Igaki H, Tachimori Y, Osugi H, Nagino M and Ushijima T.	J Cancer Res Clin Oncol,	141:453-463 (2015).	国外
Comprehensive DNA methylation and extensive mutation analyses of HER2-positive breast cancer.	Yamaguchi T, Mukai H, Yamashita S, Fujii S and Ushijima T.	Oncology	online.	国外
Establishment of a DNA Methylation Marker to Evaluate Cancer Cell Fraction in Gastric Cancer.	Zong L, Hattori N, Yoda Y, Yamashita S, Takeshima H, Takahashi T, Maeda M, Katai H, Nanjo S, Ando T, Seto Y, and Ushijima T.	Gastric Cancer	in press	国外
Identification of coexistence of DNA methylation and H3K27me3 specifically in cancer cells as a promising target for epigenetic therapy	Takeshima H, Wakabayashi M, Hattori N, Yamashita S, Ushijima T.	Carcinogenesis.	2014 Dec 4.	国外

Comparative outcomes between initially unresectable and recurrent cases of advanced pancreatic cancer following palliative chemotherapy.	Xue P, Kanai M, Mori Y, Nishimura T, Uza N, Kodama Y, Kawaguchi Y, Takaori K, Matsumoto S, Uemoto S, Chiba T.	Pancreas.	2014 Apr;43(3):411-6.	国外
Therapeutic application of curcumin for patients with pancreatic cancer	Kanai M.	World Journal of Gastroenterology	2014 in press	国外
Neutrophil-to-Lymphocyte Ratio for Predicting Palliative Chemotherapy Outcomes in Advanced Pancreatic Cancer Patients	Xue P, Kanai M, Mori Y, Nishimura T, Uza N, Kodama Y, Kawaguchi Y, Takaori K, Matsumoto S, Uemoto S, Chiba T.	Cancer Medicine	2014 Feb 12. Doi: 1002/cam4.204	国外
Fibrogenesis in alcoholic liver disease.	Fujii H, Kawada N.	World J Gastroenterol.	2014 Jul 7;20(25):8048-54.	国外
Branched-chain amino acids prevent hepatocarcinogenesis and prolong survival of patients with cirrhosis.	[illegible] Shiraishi K, Ito T, Suzuki K, Koreeda C, Ohtake T, Iwasa M, Tokumoto Y, Endo R, Kawamura NH, Shiraki M, Habu D, Tsuruta S, Miwa Y, Kawaguchi A, Kakuma T, Sakai H, Kawada N, Hanai T, Takahashi S, Kato A, Onji M, Takei Y, Kohgo Y, Seki T, Tamano M, Katayama K, [illegible]	Clin Gastroenterol Hepatol.	2014 Jun;12(6):1012-8	国外
Comparison of hepatocellular carcinoma miRNA expression profiling as evaluated by next generation sequencing and microarray.	Murakami Y, Tanahashi T, Okada R, Toyoda H, Kumada T, Enomoto M, Tamori A, Kawada N, Taguchi YH, Azuma T.	PLoS One.	2014 Sep 12;9(9):e106314.	国外
Universal disease biomarker: can a fixed set of blood microRNAs diagnose multiple diseases?	Taguchi YH, Murakami Y.	BMC Res Notes	2014 Aug 30;7:581.	国外
Role of hepatitis B virus DNA integration in human hepatocarcinogenesis.	Hai H, Tamori A, Kawada N.	World J Gastroenterol.	2014 May 28;20(20):6236-43	国外
Prospective long-term study of hepatitis B virus reactivation in patients with hematologic malignancy.	Tamori A, Hino M, Kawamura E, Fujii H, Uchida-Kobayashi S, Morikawa H, Nakamae H, Enomoto M, Murakami Y, Kawada N.	J Gastroenterol Hepatol	2014 Sep;29(9):1715-21.	国外
Clinical and pathological features of five-year survivors after pancreatectomy for pancreatic adenocarcinoma.	Kimura K, Amano R, Nakata B, Yamazoe S, Hirata K, Murata A, Miura K, Nishio K, Hirakawa T, Ohira M, Hirakawa K.	World J Surg Oncol.	2014 Nov 27;12:360	国外
Predictive factors for change of diabetes mellitus status after pancreatectomy in preoperative diabetic and nondiabetic patients.	Hirata K, Nakata B, Amano R, Yamazoe S, Kimura K, Hirakawa K.	J Gastrointest Surg.	2014 Sep;18(9):1597-603.	国外

Journal of Gastroenterology and Hepatology JGHF

doi:10.1111/jgh.12611

HEPATOLOGY

Positioning of ^{18}F-fluorodeoxyglucose-positron emission tomography imaging in the management algorithm of hepatocellular carcinoma

Etsushi Kawamura,* Susumu Shiomi,† Kohei Kotani,† Joji Kawabe,† Atsushi Hagihara,* Hideki Fujii,* Sawako Uchida-Kobayashi,* Shuji Iwai,* Hiroyasu Morikawa,* Masaru Enomoto,* Yoshiki Murakami,* Akihiro Tamori* and Norifumi Kawada*

Departments of *Hepatology and †Nuclear Medicine, Graduate School of Medicine, Osaka City University, Osaka, Japan

Key words
Barcelona Clinic Liver Cancer staging, extrahepatic metastases, FDG PET, liver cancer, treatment algorithm.

Accepted for publication 19 March 2014.

Correspondence
Dr Norifumi Kawada, Department of Hepatology, Graduate School of Medicine, Osaka City University, 1-4-3 Asahimachi, Abeno-ku, Osaka 545-8585, Japan. Email: kawadanori@med.osaka-cu.ac.jp

Conflict of Interest Statement
The authors have no conflicts of interest to disclose.

Abstract

Background and Aim: ^{18}F-fluorodeoxyglucose (FDG)-positron emission tomography (PET) may detect primary lesions (PLs) and extrahepatic metastases (EHMs) only in advanced hepatocellular carcinoma (HCC) patients. We investigated the requirement of PET and the optimal timing of PET scanning for accurate staging and treatment planning.
Methods: We conducted a retrospective investigation of 64 HCC patients who underwent PET (median age, 74 years; male/female, 41/23; etiology, 46 hepatitis C virus/4 hepatitis B virus/4 alcoholic/10 others). To determine the best timing for PET examinations, we analyzed PET result-based recommended treatment changes and characteristics of patients with FDG-avid PLs or EHMs.
Results: FDG-avid PLs were detected by PET in 22 patients (34%): 18 with hypervascular PL, 11 with serum α-fetoprotein levels ≥ 200 ng/mL, and 11 beyond Milan criteria. EHMs were detected in 21 patients (33%: lymph nodes, 8; lung, 5; abdominal wall, 4; bone, 3; other organs, 4 [including overlapping]). Recommended treatments changed for 16 patients (25%) because of Barcelona Clinic Liver Cancer stage increases based on PET scanning. In multivariate analyses, serum α-fetoprotein levels ≥ 200 ng/mL and beyond Milan criteria were independent factors for FDG-avid PLs and a maximum standardized uptake value (SUVmax) of PLs of ≥ 4.0 was an independent factor for FDG-avid EHMs ($P = 0.002$, 0.008, and 0.045, respectively).
Conclusions: PET allows detection of HCC spread in patients with elevated serum α-fetoprotein levels or those beyond Milan criteria and detects EHMs in patients with PLs with high SUVmax values. Optimally timed PET scans can complement conventional imaging for accurate staging and treatment strategy determination.

Introduction

Hepatocellular carcinoma (HCC) is one of the most common malignancies in East Asia, Scandinavia, and North America.[1] Recent advances in the treatment of HCC have led to extended life span of patients, and the number of those with extrahepatic metastases (EHMs) has been increasing.[2] Although the rate of EHM is as low as 2% in initial occurrences of HCC, patients with advanced and recurrent HCC who have received any treatment have a 20% incidence of EHM.[3] In the treatment algorithms for HCC used in Europe,[4] the United States,[5] and Japan,[6] which are constructed based on the Barcelona Clinic Liver Cancer (BCLC) stage, radical treatments such as liver resection, ablation, and transplantation are not indicated for patients with EHM. Previously, only supportive care was recommended for these patients. Currently, however, the molecular-targeted agent sorafenib has become an additional option. Therefore, the accurate clinical staging of HCC has become increasingly important to determine which patients may benefit from such newly available treatment options.

Single small HCC nodules could be detected by regular screening of high-risk patients at a 3- or 6-month interval using serum tumor marker measurements and abdominal ultrasonography with additional dynamic computed tomography (CT) and/or magnetic resonance imaging (MRI).[7] In addition, use of contrast-enhanced ultrasonography[8] and gadolinium-ethoxybenzyl-diethylenetriamine pentaacetic acid-enhanced MRI[9] has recently increased the possibility of detection of intrahepatic HCC primary lesions (PLs) in early stages. On the other hand, very few studies have examined the surveillance of EHM in patients with advanced stage HCC.

Although ^{18}F-fluorodeoxyglucose (FDG)-positron emission tomography (PET) is not useful for the diagnosis of

well-differentiated, early-stage HCC because of variable FDG uptake in hepatocytes,[10] it can detect PLs of moderate to poor differentiation, advanced-stage HCC, and EHMs, in a one-time, noninvasive whole-body scan.[11]

PET scanning has been increasingly used in patients with HCC, but its diagnostic accuracy in these cases has not yet been fully evaluated. Additionally, the question of how frequently PET results change the recommended treatment strategy has not been answered. Because PET examination is costly and not suitable for repeated evaluations, it is important to define the characteristics of HCC patients with FDG-avid PLs or FDG-avid EHMs in order to determine when PET should be performed for accurate staging of HCC.

In this study, we analyzed (i) the sensitivity, specificity, and accuracy of PET for HCC patients; (ii) the frequency of changes in recommended treatments for HCC based on PET results; and (iii) the clinical characteristics of HCC patients with FDG-avid PLs or EHMs.

Methods

Patients. A retrospective cohort study was performed to analyze 64 HCC cases in outpatients at Osaka City University Hospital who underwent PET/CT between April 2005 and November 2012. Of the 64 patients, 25 were diagnosed as having HCC by examination of liver specimens obtained by liver resection or needle biopsy performed under ultrasonographic guidance. The remaining 39 patients were clinically diagnosed with HCC by a team of three or more hepatologists based on the findings of contrast-enhanced CT or contrast-enhanced MRI and serum tumor marker levels. We examined multiple parameters related to the background of the HCC patients including age, sex, Child-Pugh score, vascularity of the PL, Milan criteria,[12] BCLC stage,[13] serum levels of α-fetoprotein (AFP), and des-γ-carboxy prothrombin (DCP). Exclusion criteria for the present study were as follows those can influence FDG avidity: fasting blood glucose on the day of PET examination of 150 mg/dL or more, or diabetes mellitus treated with insulin; past treatments, such as liver resection, interventional radiological procedures, percutaneous local ablation, or sorafenib administration within 1 month of the PET examination. The baseline characteristics of the patients are shown in Table 1. Child class, tumor markers, vascularity of PL, and BCLC stage were assessed using data measured within 1 month prior to PET/CT examinations. Chest radiography and abdominal contrast enhanced-CT (or MRI) were performed in all subjects within 3 months and 1 month prior to PET/CT examinations, respectively. We verified EHMs diagnosed on the basis of PET/CT by CT (or MRI, appropriately with contrast agent) of the chest or pelvis as necessary. Images were reviewed by 2 or more board-certified radiologists and nuclear medicine specialists each. We recorded the accuracy of diagnosis of the PL or EHM, the PET parameter of maximal standardized uptake (SUVmax) of the PL, and the rate of change of BCLC-recommended treatments according to the results of PET. We performed multivariate analyses to determine the factors associated with detection of FDG-avid PLs or EHMs. We also performed a univariate analysis of risk factors associated with overall survival after PET examination.

The clinical use of FDG PET for patients with HCC was permitted by the ethics committee of our university (approval number: 0049). The present study was performed based on their approval. Before performing PET/CT, the purpose of the diagnostic tool was explained to each patient and informed consent was obtained. Procedures of this study were in accordance with the principles outlined in the Helsinki Declaration of 1964 (2008 revision).

Table 1 Clinical characteristics of the hepatocellular carcinoma patients before ^{18}F-fluorodeoxyglucose-positron emission tomography examination

	No. of patients
Total patients	64
Age, < 65/≥ 65	11/53
Female/male	23/41
Etiology, HBV/HCV/NASH/alcohol/autoimmune/NA	4/46/3/4/1/6
Chronic hepatitis/cirrhosis, Child-Pugh class A/B/C	14/36/13/1
α-fetoprotein level (ng/mL), < 200/≥ 200/NA	41/17/6
Des-γ-carboxy prothrombin level (mAU/mL), < 150/≥ 150/NA	31/19/14
Initial occurrence/recurrence (prior treatment, TACE or TAI/ablation†/resection/sorafenib/other)	7/57 (25/16/6/8/2)
Vascularity of primary lesion‡, not hypervascular/hypervascular/NA	20/36/8
Histological differentiation, well/moderately to poorly/combined/NA	5/16/4/39
Milan criteria, within/beyond/NA	43/13/8
Barcelona Clinic Liver Cancer stage, 0/A1-4/B/C/D	15/26/10/12/1

†Radiofrequency ablation or percutaneous ethanol injection.
‡Diagnosed by contrast enhanced-computed tomography (or contrast enhanced-magnetic resonance imaging) of the liver.
HBV, hepatitis B virus; HCV, hepatitis C virus; NA, not available; NASH, nonalcoholic steatohepatitis; TACE, transcatheter arterial chemoembolization; TAI, transcatheter arterial infusion chemotherapy.

^{18}F-FDG PET scanning and data analysis. Studies were performed with PET (Eminence SET-3000B/L, Shimadzu, Kyoto, Japan) plus CT between April 2005 and May 2010. A PET-CT scanner (Biograph 16, Siemens, Bayern, Germany) was also used in a random order between June 2010 and November 2012. Whole-body images were obtained 50 min after intravenous injection of 185–370 MBq of FDG (FDG scan Injectable [Nihon Medi-physics, Tokyo, Japan] or a product in our hospital using a 12 MeV cyclotron [JFE, Tokyo, Japan]). Patients fasted for at least 4 h before the PET scan. PET plus CT fusion images were acquired on a workstation (between April 2005 and February 2010: Eminence workstation Rev02.50.12, Shimadzu, Kyoto, Japan; between March 2010 and November 2012: XTREK Browser version 1.01.16j, J-MAC Systems, Sapporo, Japan). For quantitative evaluation, a region of interest (ROI: 5 mm in diameter) was placed over the area of strong activity within the lesion, and the SUVmax was obtained by dividing the maximum activity concentration in the lesion [Bq/g] by the administrated activity [Bq/bodyweight (g)].[14] For patients with multiple PLs, the SUVmax of the largest lesion was used for statistical analysis.

Statistical analysis. The Fisher's exact test was used to compare categorical variables. Multivariate logistic regression

analyses were used for FDG-avid lesions. Univariate Cox regression was used to analyze overall survival. A P-value of less than 0.05 was considered significant. All statistical analyses were performed using JMP 9.0.3 software (SAS Institute Inc., Cary, NC, USA).

Results

The accuracy of PET for the diagnosis of PLs or EHMs is shown in Table 2. PL were detected by PET with 36% sensitivity, 100% specificity, 39% accuracy, 100% positive predictive value, and 7% negative predictive value (Fisher's exact test, $P = 0.276$), and EHMs were detected with 88% sensitivity, 75% specificity, 80% accuracy, 68% positive predictive value, and 91% negative predictive value ($P < 0.0001$).

PET detected EHMs in 21 of the 64 patients (33%) (lymph nodes in 8, the lung in 5, the abdominal wall in 4, bone in 3, and others in 4, including patients with multiple metastases). Three of these 21 patients had overlapping as follows: lung and abdominal lymph node, lung and abdominal wall, and bone and abdominal wall. The diagnostic sensitivities for the lymph nodes, lungs, abdominal wall, and bone were 80% (8/10), 83% (5/6), 80% (4/5), and 100% (3/3), respectively. The number of patients with BCLC stage 0 disease decreased from 15 to 9, that of patients with stage A disease decreased from 26 to 19, that of patients with stage B disease decreased from 10 to 7, that of patients with stage C disease increased from 12 to 28, and that of patients with stage D disease remained 1, when modified according to the results of PET. Thus, recommended treatments for HCC, based on the algorithm, were changed in 16 of the 64 patients (25%) (Fig. 1).

Multivariate logistic regression analyses of risk factors for FDG-avid PL and EHM are shown in Table 3. Because of the lack of definitive evidence indicating the proper cut-off values of AFP and DCP to predict the occurrence of PL or EHM, we used an AFP of 200 ng/mL and a DCP of 150 mAU/mL, as established by the HALT-C trial.[15] Serum levels of AFP ≥ 200 ng/mL (odds ratio [OR] 11.2, $P = 0.002$) and beyond Milan criteria (OR 10.5, $P = 0.008$) were independent factors for FDG-avid PL detection. The receiver operating characteristic analyses indicate that the best performance of SUVmax of the PL for predicting FDG-avid EHM detection and overall survival is with a cut-off of 4.0. An SUVmax of the PL ≥ 4.0 was only an independent factor for FDG-avid EHM detection (OR 4.3, $P = 0.045$). The univariate Cox regression analysis of risk factors associated with overall survival after PET examination is shown in Table 4. An SUVmax of PL ≥ 4.0 was the only independent factor significantly associated with overall survival (hazard ratio: 5.9, $P < 0.001$). Mean survival time was shorter in the group with an SUVmax of PL ≥ 4.0 ($n = 14$) than in the group with an SUVmax of PL < 4.0 ($n = 50$) (7.8 and 18.6 months, respectively).

PET/CT images of representative HCC patients with FDG-avid EHMs are shown in Figure 2. A 74-year-old woman with hepatitis

Table 2 Diagnostic accuracy of the primary lesion or extrahepatic metastases using FDG-positron emission tomography

	(A) Primary lesion			(B) Extrahepatic metastases‡		
Type of accumulation pattern	Viability† (+)	Viability† (–)	Total	Yes	No	Total
FDG avidity (+)	22	0	22	21	10	31
FDG avidity (–)	39	3	42	3	30	33
Total	61	3	64	24	40	64

(A) Sensitivity: 36%; specificity: 100%; accuracy: 39%; positive predictive value: 100%; negative predictive value: 7% ($P = 0.276$, Fisher's exact test).
(B) Sensitivity: 88%; specificity: 75%; accuracy: 80%; positive predictive value: 68%; negative predictive value: 91% ($P < 0.0001$). †Based on contrast enhanced-computed tomography (CT) (or contrast enhanced-magnetic resonance imaging [MRI]) of the liver.
‡Based on any typical imaging (e.g. chest radiography and CT [MRI] of the chest, abdomen, or pelvis).
FDG, ^{18}F-fluorodeoxyglucose.

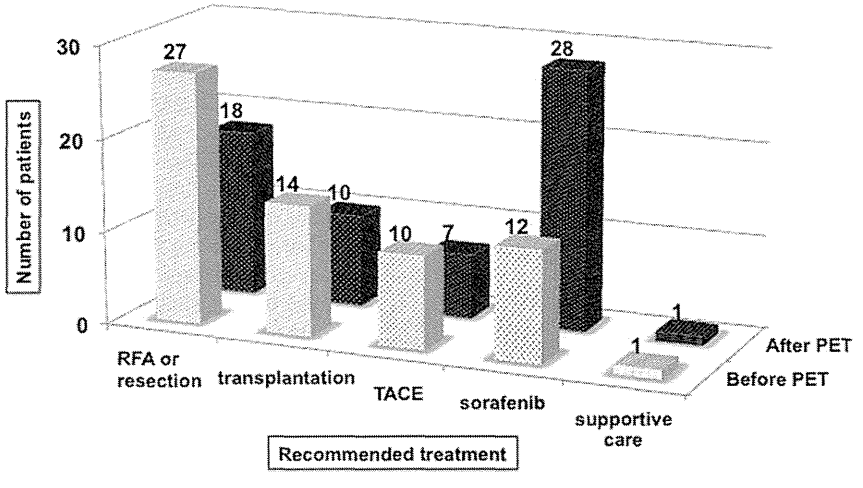

Figure 1 The distribution of patients according to the recommended treatment for hepatocellular carcinoma based on an algorithm involving Barcelona Clinic Liver Cancer stage before and after modification according to the ^{18}F-fluorodeoxyglucose-positron emission tomography (PET) results. The rate at which recommended treatment changed after PET was 25% (16/64: decrease in the summation of four treatments in 16 patients [RFA, radiofrequency ablation or resection; transplantation; and TACE, transcatheter arterial chemoembolization], increase in sorafenib in 16 patients).

Table 3 Multivariate logistic regression analyses of risk factors for FDG-avid primary lesions and extrahepatic metastases

Risk factor	For FDG-avid primary lesion						For FDG-avid extrahepatic metastases					
	COR	95% CI	*P* value	AOR	95% CI	*P* value	COR	95% CI	*P* value	AOR	95% CI	*P* value
≥ 65, years old	0.57	0.15–2.21	0.403				0.83	0.22–3.51	0.784			
Male	0.45	0.15–1.29	0.137				0.71	0.25–2.11	0.538			
Hypervascular primary lesion	4.00	1.20–16.12	0.024*	1.49	0.28–9.43	0.646	1.05	0.34–3.40	0.934	1.16	0.26–5.80	0.847
AFP level ≥ 200, ng/mL	5.68	1.73–20.53	0.004*	11.19	2.42–69.40	0.002*	1.51	0.46–4.86	0.493	0.99	0.24–3.74	0.992
DCP level ≥ 150, mAU/mL	2.49	0.72–8.90	0.147				1.06	0.32–3.47	0.923			
Beyond Milan criteria	8.61	2.21–43.65	0.002*	10.45	1.77–92.03	0.008*	1.44	0.38–5.21	0.582	0.79	0.14–3.85	0.771
SUVmax of primary lesion ≥ 4.0							3.80	1.12–13.62	0.032*	4.31	1.04–20.07	0.045*

*$P < 0.05$.

AFP, α-fetoprotein; AOR, adjusted odds ratio; CI, confidence interval; COR, crude odds ratio; DCP, des-γ-carboxy prothrombin; FDG, ^{18}F-fluorodeoxyglucose; SUVmax, maximum standardized uptake value.

Table 4 Univariate Cox regression analysis of risk factors for overall survival after ^{18}F-fluorodeoxyglucose-positron emission tomography examination

Risk factor	Crude hazard ratio	95% Confidence interval	*P* value
≥ 65, years old	0.87	0.29–3.70	0.820
Male	0.76	0.33–1.78	0.512
Hypervascular primary lesion	1.79	0.70–5.47	0.237
AFP level ≥ 200, ng/mL	1.28	0.45–3.23	0.628
DCP level ≥ 150, mAU/mL	1.97	0.75–5.04	0.166
Beyond Milan criteria	1.71	0.60–4.30	0.295
SUVmax of primary lesion ≥ 4.0	5.91	2.39–14.58	< 0.001*

*$P < 0.05$.

AFP, α-fetoprotein; DCP, des-γ-carboxy prothrombin; SUVmax, maximum standardized uptake value.

B virus (HBV)-related cirrhosis was diagnosed with HCC approximately 6 months before PET examination, and was treated with transcatheter arterial chemoembolization (TACE). She had multinodular HCC that was approximately 9 cm at its maximum diameter and her Child-Pugh class was B. The PET examination revealed EHM on her abdominal wall (Fig. 2a). A 64-year-old man with HBV-related HCC had been treated several times with TACE and other treatments during the 14 years after his primary diagnosis. He had multinodular HCC that was approximately 3 cm at its maximum diameter, and his Child-Pugh class was B. The PET examination showed right iliac bone metastasis (Fig. 2b). In both cases, the BCLC stage was B before PET, which was changed to stage C based on the FDG-avid EHM. Accordingly, the recommended treatment was changed from TACE to sorafenib.

Discussion

PET using ^{18}F-FDG has been established as a noninvasive tool for the diagnosis of various malignancies. It is considered a useful imaging method for tumor characterization, tumor staging, and assessment of therapy response.[16–18] Although it is recognized that the sensitivity of PET scans is insufficient in cases of HCC with low malignant potential (well-differentiated), PET is important for disease staging and prognosis prediction in cases of HCC with high malignant potential (moderately to poorly differentiated).[19,20] The liver is known to have high activity of glucose 6-phosphatase (G6Pase).[21] The G6Pase activity of low malignant potential HCC tends to be higher than that of high malignant potential HCC, suggesting that low malignant potential HCC may retain the properties of normal liver tissue. In contrast, assessment of glucose metabolism to help stage patients with high malignant potential HCC has been reported.[10] In addition, in the present study, we found that the detection sensitivity of PET for PL is low in patients with HCC of various grades, compared with the sensitivity for EHM detection (Table 2).

Additional metastatic HCC cases were detected by PET, resulting in alteration of the recommended treatment (mostly from curative treatment to sorafenib) in 25% of all patients because of the increase in the BCLC stage as shown in Figure 1. PET is beneficial for proper identification of patients in whom sorafenib is indicated. It is important to note that when EHMs are undetected after FDG PET, this should be confirmed by high-quality diagnostic imaging modalities such as multidetector CT and MRI. This is because we must be aware that the PET results are not always accurate. In this study, PET results had a 13% false negative rate (3/24), and a 25% false positive rate (10/40) for the detection of EHMs (Table 2). On the other hand, of the 21 patients who had EHMs detected by PET in the present study, three patients had multiple metastases in different sites. Thus, PET is advantageous because it can detect tumors in different organs in a one-time systemic scan.

It is well established that advanced intrahepatic lesions with elevated levels of serum tumor markers are risk factors for EHM.[22] The present study proposed that an AFP level ≥ 200 ng/mL and being beyond Milan criteria can be used to indicate the appropriate time to screen patients using PET examinations (Table 3). DCP was not an independent predictive factor of FDG-avid PL or FDG-avid EHM detection, even when we used 40, 100, and 200 mAU/mL as cut-off values (Supporting Information Table S1). A corollary study is needed to determine whether a high AFP level is associated with a specific subtype of HCC. Table 3 also

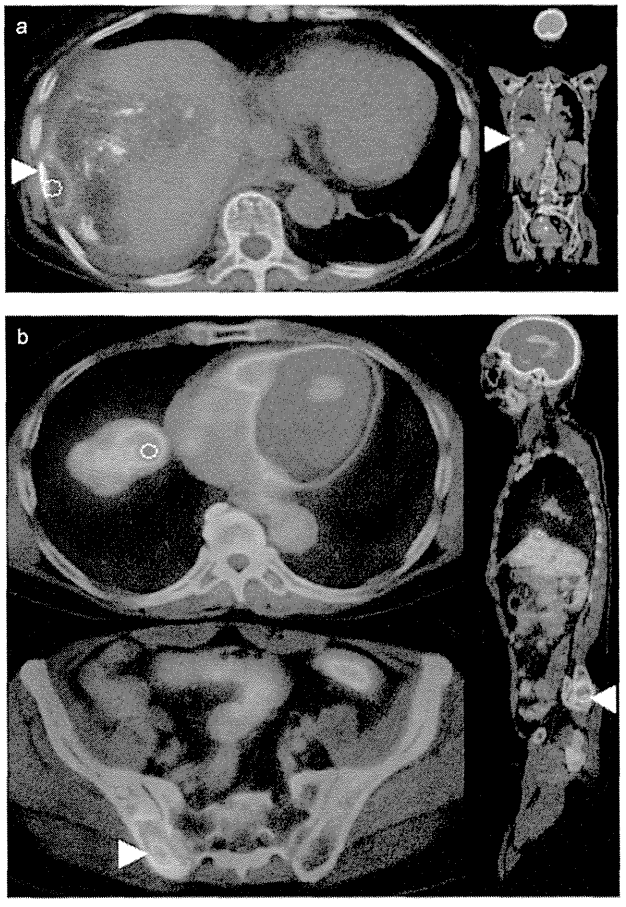

Figure 2 ^{18}F-fluorodeoxyglucose (FDG)-positron emission tomography/computed tomography of two patients with hepatocellular carcinoma with FDG-avid primary lesion (PL) and extrahepatic metastases (EHM) detection. (a) A 74-year-old woman with hepatitis B virus-related cirrhosis: hypervascular PL with maximum standardized uptake value (SUVmax) of 7.2 (≥ 4.0, white circle) with EHM (abdominal wall invasion, arrowhead); abdominal axial and whole-body coronal images. The risk factors of FDG-avid PL were as follows: α-fetoprotein (AFP) level of 19.3 ng/mL and beyond Milan criteria. (b) A 64-year-old man with hepatitis B virus-related cirrhosis: hypervascular PL with SUVmax of 4.2 (≥ 4.0, white circle) with EHM (right iliac bone, arrowhead); thoracic axial, sacrum axial, and whole-body sagittal images. The risk factors for FDG-avid PL were as follows: AFP level of 18.8 ng/mL and beyond Milan criteria.

proposes that a PL with an SUVmax ≥ 4.0 is a significant predictive factor for EHM. It is reasonable that PET detected EHM at a high rate in the patients who had PL with strong glucose metabolism. The SUVmax of PL ≥ 4.0 is considered to correlate with the malignant potential of the PL, corresponding to moderately to poorly differentiated HCC.[23] Moreover, Table 4 indicates that the PET results, such as PL with a high SUVmax, play an important role in predicting prognosis in high malignant potential HCC.

The organs where PET imaging detected EHM were the lymph node, lung, abdominal wall, and bone, as mentioned in the results. Generally speaking, a metastatic lymph node is considered to be of significant size if it is 10 mm or more along the minor axis. PET has been shown to detect lesions of 10 mm or more in diameter with high malignancy.[24] However, in PET-CT fusion images, a gap between PET images and CT images occurs in association with respiratory fluctuation, making it difficult to detect small metastatic lesions, especially in the lower lung field.[25] As shown in Figure 2a, abdominal wall invasion with high FDG uptake is detectable by PET, even when it is not detected on CT, MRI, and ultrasonography because of low volume. Because bone metastases from HCC are generally osteolytic, bone scintigraphy is not useful for detection.[26] In fact, Figure 2b shows that PET is able to reveal a bone metastasis that was not depicted by bone scintigraphy.[27]

One limitation of the present study was the lack of sufficient whole-body search for EHM using conventional imaging (radiography, CT, and MRI) prior to PET examination of all subjects. This occurred because of the lack of precise rules related to screening for EHM. The positive merit of routine screening by chest CT and bone scintigraphy in HCC within Milan criteria is low.[28] Another limitation is that this study was conducted in patients with heterogeneous tumor stages and prior treatments.[29] It was difficult to select patients of a specific clinical background because a limited number of patients with HCC underwent PET examination in clinical practice. Further validation studies are needed.

In summary, PET gives hepatologists additional screening information about PL and EHM in HCC, and this information effects the indications for radical treatment or sorafenib intervention. We believe that our study is the first to provide evidence that HCC patients with serum AFP levels ≥ 200 ng/mL or those beyond Milan criteria are good candidates for PET examinations to evaluate the spread of the lesion. Importantly, EHM could be detected at a high rate in patients who had PL with SUVmax ≥ 4.0. PET performed at the correct time is beneficial to complement conventional imaging methods in BCLC staging and determination of optimal treatment.

Acknowledgments

The authors wish to thank the staff of the Departments of Hepatology and Nuclear Medicine of Osaka City University Hospital for providing their valuable assistance and PET scanner time during this study.

References

1 Parkin DM, Bray F, Ferlay J, Pisani P. Estimating the world cancer burden: Globocan 2000. *Int. J. Cancer* 2001; **94**: 153–6.
2 Poon RT, Fan ST, Lo CM *et al.* Improving survival results after resection of hepatocellular carcinoma: a prospective study of 377 patients over 10 years. *Ann. Surg.* 2001; **234**: 63–70.
3 Uchino K, Tateishi R, Shiina S *et al.* Hepatocellular carcinoma with extrahepatic metastasis: clinical features and prognostic factors. *Cancer* 2011; **117**: 4475–83.
4 European Association for the Study of the Liver; European Organisation for Research and Treatment of Cancer. EASL-EORTC clinical practice guidelines: management of hepatocellular carcinoma. *J. Hepatol.* 2012; **56**: 908–43.
5 Bruix J, Sherman M. American Association for the Study of Liver Diseases. Management of hepatocellular carcinoma: an update. *Hepatology* 2011; **53**: 1020–2.

6 Kudo M, Izumi N, Kokudo N *et al.* Management of hepatocellular carcinoma in Japan: Consensus-Based Clinical Practice Guidelines proposed by the Japan Society of Hepatology (JSH) 2010 updated version. *Dig. Dis.* 2011; **29**: 339–64.
7 Trinchet JC, Chaffaut C, Bourcier V *et al.* Ultrasonographic surveillance of hepatocellular carcinoma in cirrhosis: a randomized trial comparing 3- and 6-month periodicities. *Hepatology* 2011; **54**: 1987–97.
8 Arita J, Hasegawa K, Takahashi M *et al.* Correlation between contrast-enhanced intraoperative ultrasound using Sonazoid and histologic grade of resected hepatocellular carcinoma. *AJR Am. J. Roentgenol.* 2011; **196**: 1314–21.
9 Haradome H, Grazioli L, Tinti R *et al.* Additional value of gadoxetic acid-DTPA-enhanced hepatobiliary phase MR imaging in the diagnosis of early-stage hepatocellular carcinoma: comparison with dynamic triple-phase multidetector CT imaging. *J. Magn. Reson. Imaging* 2011; **34**: 69–78.
10 Trojan J, Schroeder O, Raedle J *et al.* Fluorine-18 FDG positron emission tomography for imaging of hepatocellular carcinoma. *Am. J. Gastroenterol.* 1999; **94**: 3314–19.
11 Sugiyama M, Sakahara H, Torizuka T *et al.* ^{18}F-FDG PET in the detection of extrahepatic metastases from hepatocellular carcinoma. *J. Gastroenterol.* 2004; **39**: 961–8.
12 Mazzaferro V, Regalia E, Doci R *et al.* Liver transplantation for the treatment of small hepatocellular carcinomas in patients with cirrhosis. *N. Engl. J. Med.* 1996; **334**: 693–9.
13 Llovet JM, Di Bisceglie AM, Bruix J *et al.* Design and endpoints of clinical trials in hepatocellular carcinoma. *J. Natl Cancer Inst.* 2008; **100**: 698–711.
14 Strauss LG, Conti PS. The applications of PET in clinical oncology. *J. Nucl. Med.* 1991; **32**: 623–48; discussion 49–50.
15 Sterling RK, Wright EC, Morgan TR *et al.* Frequency of elevated hepatocellular carcinoma (HCC) biomarkers in patients with advanced hepatitis C. *Am. J. Gastroenterol.* 2012; **107**: 64–74.
16 Rigo P, Paulus P, Kaschten BJ *et al.* Oncological applications of positron emission tomography with fluorine-18 fluorodeoxyglucose. *Eur. J. Nucl. Med.* 1996; **23**: 1641–74.
17 Giannopoulou C. The role of SPET and PET in monitoring tumour response to therapy. *Eur. J. Nucl. Med. Mol. Imaging* 2003; **30**: 1173–200.
18 Hiraoka A, Hirooka M, Ochi H *et al.* Importance of screening for synchronous malignant neoplasms in patients with hepatocellular carcinoma: impact of FDG PET/CT. *Liver Int.* 2013; **33**: 1085–91.
19 Shiomi S, Kawabe J. Clinical applications of positron emission tomography in hepatic tumors. *Hepatol. Res.* 2011; **41**: 611–17.
20 Pant V, Sen IB, Soin AS. Role of ^{18}F-FDG PET CT as an independent prognostic indicator in patients with hepatocellular carcinoma. *Nucl. Med. Commun.* 2013; **34**: 749–57.
21 Gallagher BM, Fowler JS, Gutterson NI, MacGregor RR, Wan CN, Wolf AP. Metabolic trapping as a principle of oradiopharmaceutical design: some factors resposible for the biodistribution of [^{18}F] 2-deoxy-2-fluoro-D-glucose. *J. Nucl. Med.* 1978; **19**: 1154–61.
22 Kanda M, Tateishi R, Yoshida H *et al.* Extrahepatic metastasis of hepatocellular carcinoma: incidence and risk factors. *Liver Int.* 2008; **28**: 1256–63.
23 Seo S, Hatano E, Higashi T *et al.* Fluorine-18 fluorodeoxyglucose positron emission tomography predicts tumor differentiation, P-glycoprotein expression, and outcome after resection in hepatocellular carcinoma. *Clin. Cancer Res.* 2007; **13**: 427–33.
24 Morón FE, Szklaruk J. Learning the nodal stations in the abdomen. *Br. J. Radiol.* 2007; **80**: 841–8.
25 Tsukamoto E, Ochi S. PET/CT today: system and its impact on cancer diagnosis. *Ann. Nucl. Med.* 2006; **20**: 255–67.
26 Natsuizaka M, Omura T, Akaike T *et al.* Clinical features of hepatocellular carcinoma with extrahepatic metastases. *J. Gastroenterol. Hepatol.* 2005; **20**: 1781–7.
27 Kawaoka T, Aikata H, Takaki S *et al.* FDG positron emission tomography/computed tomography for the detection of extrahepatic metastases from hepatocellular carcinoma. *Hepatol. Res.* 2009; **39**: 134–42.
28 Koneru B, Teperman LW, Manzarbeitia C *et al.* A multicenter evaluation of utility of chest computed tomography and bone scans in liver transplant candidates with stages I and II hepatoma. *Ann. Surg.* 2005; **241**: 622–8.
29 European Association for the Study of the Liver, European Organisation for Research and Treatment of Cancer. EASL-EORTC clinical practice guidelines: management of hepatocellular carcinoma. *J. Hepatol.* 2012; **56**: 908–43.

Supporting information

Additional Supporting Information may be found in the online version of this article at the publisher's web-site:

Table S1 Univariate logistic regression analyses of DCP level for FDG-avid primary lesions and extrahepatic metastases.

Cancer Science
Japanese Cancer Association JCA
Open Access

Phase I study of combination chemotherapy using sorafenib and transcatheter arterial infusion with cisplatin for advanced hepatocellular carcinoma

Atsushi Hagihara,[1,2] Masafumi Ikeda,[3] Hideki Ueno,[1] Chigusa Morizane,[1] Shunsuke Kondo,[1] Kohei Nakachi,[3] Shuichi Mitsunaga,[3] Satoshi Shimizu,[3] Yasushi Kojima,[3] Eiichiro Suzuki,[3] Kazuhiro Katayama,[4] Kazuho Imanaka,[4] Chie Tamai,[4] Yoshitaka Inaba,[5] Yozo Sato,[5] Mina Kato[5] and Takuji Okusaka[1]

[1]Department of Hepatobiliary and Pancreatic Oncology, National Cancer Center Hospital, Tokyo; [2]Department of Hepatology, Osaka City University Hospital, Osaka; [3]Department of Hepatobiliary and Pancreatic Oncology, National Cancer Center Hospital East, Kashiwa; [4]Department of Hepatobiliary and Pancreatic Oncology, Osaka Medical Center for Cancer and Cardiovascular Diseases, Osaka; [5]Department of Diagnostic and Interventional Radiology, Aichi Cancer Center Hospital, Aichi, Japan

Key words
Arterial infusion, chemotherapy, cisplatin, hepatocellular carcinoma, sorafenib

Correspondence
Masafumi Ikeda, Department of Hepatobiliary and Pancreatic Oncology, National Cancer Center Hospital East, 6-5-1 Kashiwanoha, Kashiwa, Chiba 277-8577, Japan.
Tel: +81-4-7133-1111; Fax: +81-4-7133-0335;
E-mail: masikeda@east.ncc.go.jp

Funding information
Ministry of Health, Labour and Welfare, Japan.

Received November 12, 2013; Revised January 10, 2013; Accepted January 12, 2014

Cancer Sci (2014)

doi: 10.1111/cas.12353

The aims of this study were to evaluate the frequency of dose-limiting toxicities and to find the recommended dose of combination chemotherapy with sorafenib and transcatheter arterial infusion (TAI) using cisplatin for patients with advanced hepatocellular carcinoma (HCC), for whom surgical resection, local ablation therapy, or transcatheter arterial chemoembolization were not indicated. Patients received 800 mg sorafenib daily. Cisplatin was given at one of three dosages (level 1, 35 mg/m^2/cycle; level 2, 50 mg/m^2/cycle; and level 3, 65 mg/m^2/cycle) from feeding arteries to the HCC. The treatment was repeated every 4–6 weeks up to a maximum of six cycles, until there were signs of tumor progression or unacceptable toxicity. The dose-limiting toxicities experienced by the 20 enrolled patients were grade 4 increased aspartate aminotransferase at level 1, grade 3 gastrointestinal hemorrhaging at level 1, and grade 3 hypertension at level 3. The common drug-related adverse events that were of severity grade 3 or 4 included the elevation of aspartate aminotransferase (30%), alanine aminotransferase (20%), amylase (30%), and lipase (30%). Partial response was seen in four patients (20%), and 13 patients (65%) had stable disease. The median overall survival and progression-free survival were 9.1 and 3.3 months, respectively. The combination of sorafenib at 800 mg/day with TAI of cisplatin at 65 mg/m^2/cycle was determined to be the recommended regimen. A randomized phase II trial of sorafenib alone versus sorafenib plus TAI of cisplatin is currently underway. This study was registered at UMIN as trial number UMIN000001496.

Hepatocellular carcinoma is one of the most common types of cancer worldwide.[1] Hepatic resection, liver transplantation, and local ablation therapy, including radiofrequency ablation and percutaneous ethanol injection, are considered to be curative treatments for HCC.[2–4] Transcatheter arterial chemoembolization has been recognized as an effective but non-curative treatment for patients with large or multifocal, unresectable HCC without vascular invasion or extrahepatic spread.[4] However, the majority of patients develop recurrence or metastasis after these treatments, and their HCCs progress to the advanced stages. Two separate phase III trials have reported that sorafenib, an oral multikinase inhibitor, prolongs OS with manageable toxicities.[5,6] Thus, sorafenib has been accepted as standard first-line chemotherapy for patients who cannot benefit from resection, transplantation, local ablation therapy, or TACE, and who still have preserved liver function. However, sorafenib treatment has yielded rather unsatisfactory results in terms of OS of patients with advanced HCC.

In Japan, TAI chemotherapy is often given to patients with localized advanced HCC, such as in cases with vascular invasion. Transcatheter arterial infusion likely has better antitumor activity and reduced toxicity compared to systemic chemotherapy, because TAI can increase the local concentration of anticancer drugs while reducing their systemic distribution and accompanying adverse effects.[7,8] However, TAI has not been established as a standard treatment for advanced HCC, because the survival benefit has not been evaluated in large-scale prospective randomized trials. Cisplatin alone,[9,10] 5-FU plus cisplatin,[11] and 5-FU plus interferon[12] are frequently used chemotherapeutic regimens that have been shown to lead to tumor shrinkage and increased OS. Among these options, TAI of cisplatin does not require an implanted reservoir system, so it is easier to manage its administration. In addition, favorable antitumor efficacy[10] has been reported by previous phase II trials. The combination of sorafenib and TAI of cisplatin might be more effective than sorafenib alone for the treatment of advanced HCC. Therefore, we planned a phase I study of the combination chemotherapy of sorafenib and TAI with cisplatin for advanced HCC. The primary endpoint of this trial was to determine the recommended doses of TAI of

cisplatin and sorafenib to use for combination therapy, according to the frequency of its DLT. The secondary goal of this study was to evaluate the toxicity and efficacy of this combination in patients with advanced HCC.

Materials and Methods

Patient eligibility. Patients eligible for enrolment in this study had advanced HCC for which surgical resection, local ablation therapy, and TACE were not indicated. Hepatocellular carcinoma was diagnosed by either histologic examination or based on a computed tomographic scan, angiograph, and an increased level of serum AFP or DCP. Eligibility criteria included the following factors: (i) 20–79 years of age; (ii) an Eastern Cooperative Oncology Group performance status score of 0–2; (iii) one or more measurable lesions in the liver; (iv) adequate hematological function (hemoglobin levels of 8.5 g/dL or more, neutrophil counts of 1500 cells/mm^3 or more, and platelet counts of 70 000 cells/mm^3 or more); (v) adequate hepatic function (serum total bilirubin levels of 2.0 mg/dL or less, serum albumin levels of 2.8 g/dL or more, and serum AST/ALT levels within five times the ULN, Child–Pugh score of seven points or less); (vi) adequate pancreatic function (serum total amylase/lipase levels within two times the ULN); and (vii) adequate renal function (serum creatinine level within normal limits and creatinine clearance of 60 mL/min or more). Previous local therapy for intrahepatic lesions, such as hepatic resection, percutaneous local ablation, or TACE was allowed if it had not been given within the 4 weeks before this treatment. In this study, the eligibility criterion regarding the Child–Pugh classification was set at a score of seven points or less, because sorafenib has been reported to be feasible in patients with Child–Pugh class B.[13,14]

Patients were excluded from the study if they had a treatment history of sorafenib or cisplatin for HCC, an active infection, uncontrollable hypertension, severe heart disease, refractory pleural effusion or ascites, a severe mental disorder or encephalopathy, an active gastroduodenal ulcer or esophageal bleeding, or active concomitant malignancy. This study also excluded pregnant and lactating women, women of childbearing age unless they were using effective contraception, and patients with other serious medical conditions.

Treatment plan. Sorafenib (Bayer Health Care Pharmaceuticals, West Haven, CT, USA) was given orally at a dose of 800 mg daily. Cisplatin (Nippon Kayaku, Tokyo, Japan) was concurrently administered by a catheter in the proper, right, or left hepatic artery, or another feeding artery, under angiographic guidance with the Seldinger technique on the same day as sorafenib administration at one of three dosages (35 mg/m^2/cycle for level 1, 50 mg/m^2/cycle for level 2, or 65 mg/m^2/cycle for level 3) (Table 1). The maximum dose of cisplatin was set according to the dose approved by Japanese insurance for single-use as an intra-arterial therapy.[10] The treatment was repeated every 4–6 weeks up to a maximum of six cycles, until there was evidence of tumor progression or unacceptable toxicity. A list of suspension criteria was set, and the treatment of patients receiving sorafenib that met these criteria was interrupted until the toxicities were resolved. When resuming treatment, the dose of sorafenib needed to be reduced to 400 mg daily. If additional dose reduction was required, the dose was reduced to a single 400-mg dose every other day. The suspension criteria for sorafenib were defined as: (i) grade 4 neutropenia or thrombocytopenia; (ii) grade 3 or 4 non-hematological toxicity excluding increased levels of serum AST/ALT/γ-GT, pancreatic enzyme increases, HFSR, hyperglycemia, and constipation; (iii) grade 4 pancreatic enzyme increases with clinical and/or imaging findings of pancreatitis, or a pancreatic adverse event considered to be life threatening; (iv) serum AST/ALT levels of 10 times the ULN; (v) serum creatinine levels of 2.0 mg/dL or more; (vi) grade 2 or 3 HFSR; and (vii) grade 2 or 3 hypertension.

Table 1. Dosage levels of sorafenib and cisplatin administered to patients with advanced hepatocellular carcinoma

Level	Sorafenib (mg/day)	Cisplatin TAI (mg/m^2/cycle)	Remarks
1	800	35	Starting dose
2	800	50	
3	800	65	Recommended dose

The starting criteria for cisplatin TAI were defined as follows: (i) neutrophil counts of 1200/mm^3 or more; (ii) thrombocyte counts of 50 000 cells/mm^3 or more; (iii) total bilirubin levels of 3.0 mg/dL or less; (iv) AST or ALT levels five times the ULN or less; and (v) creatinine levels of 1.5 mg/dL or less. If these adverse events were outside of the starting criteria, TAI of cisplatin was postponed until the criteria were fulfilled.

Clinical assessments. The trial was an open-label, single-arm phase I study that was carried out at four cancer centers in Japan. The primary endpoints were to evaluate the frequency of DLTs and to determine the recommended doses of sorafenib and cisplatin in a phase II study. Dose escalation followed a standard "3 plus 3" dose escalation design. In other words, at least three patients were enrolled at each of three dosage levels. If one or two DLTs were observed in the initial three patients, three additional patients were entered at the same dosage level. If DLTs were not observed in three of the three patients, or three or more of the six patients treated at that level during the first cycle of treatment, the dose of cisplatin was escalated to the next level. At the highest dosage level, three additional patients were entered and the safety was evaluated carefully during the first three cycles of the nine patients. An additional patient would be included when treatment was terminated for reasons other than DLT before the end of the first course, because it would be impossible to determine the frequency of DLTs. The efficacy and safety evaluation committee determined the recommended dose. Dose-limiting toxicities were defined as follows: (i) febrile neutropenia; (ii) grade 4 leucopenia or grade 4 neutropenia persisting for 7 days or more; (iii) grade 4 thrombocytopenia or thrombocytopenia requiring transfusion; (iv) grade 3 or 4 non-hematological toxicity excluding increased serum AST/ALT/γ-GT levels, increased pancreatic enzyme levels, HFSR, hyperglycemia, or constipation; (v) grade 4 increased pancreatic enzyme levels with clinical and/or imaging findings of pancreatitis, or a pancreatic adverse event considered to be life threatening; (vi) serum AST/ALT levels of 10 times the ULN or more; (vii) serum creatinine levels of 2.0 mg/dL or more; and (viii) any toxicities that necessitated a treatment delay of more than 4 weeks. Toxicities were graded according to the Common Terminology Criteria for Adverse Events, version 3.0. During treatment, a complete blood count with differentials, serum chemistry, and urinalysis was obtained biweekly. Tumor response was evaluated every 6 weeks using RECIST version 1.0. Progression-free survival was defined as the time from enrolment in this trial to the first documentation of progression or death. Overall survival was the time from enrolment in this

trial to the date of death or the date of the last follow-up. Both PFS and OS times were calculated using the Kaplan–Meier method.

This protocol was approved for clinical investigation by each institution's review board in accordance with the provisions of the Declaration of Helsinki, Good Clinical Practice guidelines, and local laws and regulations. Written informed consent was obtained from all patients who were considered eligible for participation in this study before enrolment. This study was registered at UMIN as trial number UMIN000001496.

Results

Patient characteristics. A total of 20 patients were enrolled in the trial between December 2008 and August 2010. The patient characteristics are listed in Table 2. Seven patients were enrolled at dose level 1, three patients at dose level 2, and 10 patients at dose level 3. This was because we replaced one more patient at dose levels 1 and 3, according to the recommendation of the efficacy and safety evaluation committee. Sorafenib treatment was terminated for one patient at dose level 1 who developed grade 3 erythema multiforme and one patient at dose level 3 who developed hypoglycemia owing to disease progression on the 11th day of the first cycle. Erythema multiforme was a distinctive adverse event of sorafenib and was therefore not considered a DLT in this study. In addition, hypoglycemia was considered unrelated to the combination therapy.

The median dose intensity of sorafenib and the median relative dose intensity were 528 mg daily and 66%, respectively (Table 3). There was no decrease in the dose of cisplatin. The median number of cycles of cisplatin was 2.8 (range, 1–6 cycles).

Table 2. Baseline characteristics of patients with advanced hepatocellular carcinoma enrolled in this study

Characteristics		Level 1	Level 2	Level 3	Total
	No. of patients	7	3	10	20
Age, years	30–39	0	0	1	1
	40–49	0	0	1	1
	50–59	1	2	1	4
	60–69	3	0	2	6
	70–79	3	1	4	8
PS	0	7	3	8	19
	1	0	0	1	1
Viral marker	HBs Ag (+)	0	1	3	5
	HCV Ab (+)	3	1	3	7
Child–Pugh score	5	4	2	4	11
	6	1	1	3	5
	7	2	0	2	4
Portal vein invasion	Vp 3	1	0	3	4
	Vp 4	3	0	2	5
Distant metastases	Absent	4	2	6	13
	Present	3	1	3	7
Stage (UICC v.6)	II	0	1	0	1
	III	4	1	6	12
	IV	3	1	3	7

HBs Ag, hepatitis B surface antigen; HCV Ab, hepatitis C antibody; PS, performance status; UICC, Union for International Cancer Control; Vp 3, hepatocellular carcinoma invasion of the first-order branch of the portal vein; Vp 4, hepatocellular carcinoma invasion of the main trunk of the portal vein.

Table 3. Dosage intensity and number of transcatheter arterial infusion (TAI) cycles in patients with advanced hepatocellular carcinoma treated with sorafenib and cisplatin

	Level 1	Level 2	Level 3	Total
No. of enrolled patients	7	3	10	20
No. of patients with dose reduction of sorafenib (%)	2 (29)	1 (33)	5 (50)	8 (40)
Mean relative dose intensity of sorafenib, %	91	78	62	66
Mean no. of cisplatin TAI cycles	3.1	1.6	3.0	2.8

Adverse events. The DLTs included grade 4 increased AST, grade 3 gastrointestinal hemorrhage, and grade 3 hypertension. At dose level 1, two of the seven patients experienced DLTs; the first of these patients developed grade 4 increased levels of serum AST on the 13th day of the first cycle, and the second patient experienced grade 3 gastrointestinal bleeding and grade 3 bacteremia on the 13th day of the first cycle. No DLTs occurred in patients receiving dose level 2. At dose level 3, one patient experienced DLT in the form of grade 3 hypertension on the 32nd day of the first cycle, but no other DLTs were seen at this dose level.

The most common grade 3 or 4 drug-related adverse events included increased levels of AST (30%), amylase (30%), lipase (30%), ALP (10%), and γ-GT (10%), anemia (15%), leukopenia (10%), and thrombocytopenia (10%) during the entire periods of the combination therapy (Table 4). There were no treatment-related deaths in this trial. Therefore, the combination therapy of TAI of cisplatin at 65 mg/m^2 with 800 mg /day sorafenib was considered to be manageable.

Tumor response and survival. No patients had a complete response, five patients (25%) showed partial responses, and 12 patients (60%) showed stable disease. Progressive disease occurred in three patients (15%). During the treatment, the serum AFP level decreased in 12 patients (60%), and the serum DCP level decreased in nine patients (45%). All patients were included in the survival assessment. Of the 20 patients, one is still alive at the time of drafting this manuscript. He survived more than 40 months. He received six courses of combination chemotherapy of sorafenib with TAI of cisplatin. His HCC shrank partially, allowing for surgical resection, and no recurrence was seen. The other 19 patients did not survive. The cause of death was tumor progression in 18 of the patients and myocardial disease in one patient. The median OS and median PFS were 9.1 and 3.3 months, respectively (Fig. 1).

Discussion

For advanced HCC patients with preserved liver function with a Child–Pugh score of A, sorafenib has been reported to prolong OS compared to placebo with manageable toxicity in two pivotal phase III trials.[5,6] However, the OS times of 10.7 months in the SHARP study and 6.5 months in the Asia-Pacific study are still unsatisfactory. Several clinical trials of sorafenib combined with systemic chemotherapy agents or novel molecular targeted agents have been carried out, but few favorable results were reported.[15] Combination chemotherapy with TAI may be a promising alternative. Transcatheter arterial infusion can increase the local concentration of anticancer drugs while reducing their systemic distribution and accompanying adverse effects.[7,8] Cisplatin is an anticancer agent that has a potency that is directly related to its concentration. The

Table 4. Adverse events observed in patients with advanced hepatocellular carcinoma treated with sorafenib and cisplatin by transcatheter arterial infusion (TAI) (n = 20)

Characteristic	Level 1						Level 2						Level 3						Total	
No. of pts	n = 7				%	%	n = 3				%	%	n = 10				%	%	%	%
Grade (CTCAE v.3.0)	1	2	3	4	Any	3/4	1	2	3	4	Any	3/4	1	2	3	4	Any	3/4	Any	3/4
Leukopenia	3	0	1	0	57	14	0	2	0	0	33	0	2	3	1	0	60	10	55	10
Neutropenia	2	0	1	0	43	14	1	1	0	0	66	0	3	1	0	0	40	0	45	5
Anemia	1	1	2	0	57	29	1	0	0	0	33	0	2	0	1	0	30	10	35	15
Thrombocytopenia	1	2	1	0	57	14	0	2	0	0	66	0	1	6	1	0	80	10	70	10
Hyperbilirubinemia	4	2	0	0	86	29	3	0	0	0	33	0	3	4	0	0	70	0	80	0
AST increased	0	2	1	1	57	29	0	1	2	0	100	66	2	6	2	0	100	20	85	30
ALT increased	1	0	2	0	43	29	1	1	1	0	100	33	2	2	1	0	50	10	55	20
γ-GT increased	0	2	0	1	43	14	0	1	0	0	33	33	0	3	1	0	40	10	40	10
ALP increased	2	0	1	0	43	14	1	1	0	0	66	0	2	1	1	0	40	10	45	10
Amylase increased	0	0	0	1	14	14	0	1	0	0	33	0	3	0	5	0	80	50	50	30
Lipase increased	0	0	0	1	14	14	1	0	1	0	66	33	2	0	1	3	60	10	45	30
Anorexia	2	1	0	0	43	0	0	0	0	0	0	0	2	1	1	0	40	10	35	5
Nausea	1	0	0	0	14	0	0	0	0	0	0	0	2	0	1	0	30	10	20	5
Hypertension	0	0	0	0	0	0	0	0	0	0	0	0	1	0	1	0	20	10	10	5
Gastrointestinal bleeding	0	0	1	0	14	14	0	0	0	0	0	0	0	0	1	0	10	10	10	10
Bacteremia	0	0	1	0	14	14	0	0	0	0	0	0	0	0	0	0	0	0	5	5

ALP, alkaline phosphatase; ALT, alanine aminotransferase; AST, aspartate aminotransferase; CTCAE, Common Terminology Criteria for Adverse Events; γ-GT, γ-glutamyl transpeptidase.

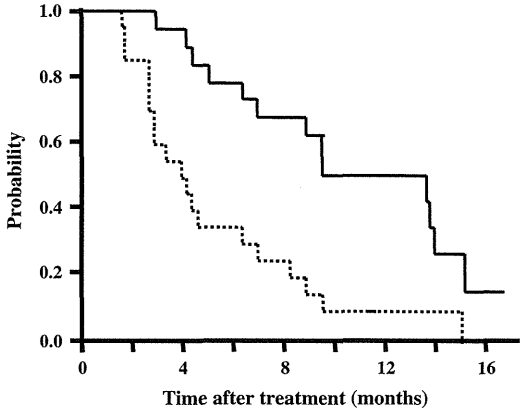

Fig. 1. Overall survival curve (solid line) and progression-free survival curve (dashed line) of all patients enrolled in this trial of sorafenib combined with transcatheter arterial infusion of cisplatin for patients with advanced hepatocellular carcinoma.

response rate to intra-arterially administered cisplatin has been reported to be 33.8%,[10] compared to a response rate of only 9% to systemically administered cisplatin.[16] Thus, intra-arterial administration of cisplatin appears to be more effective than systemic administration of cisplatin. Moreover, sorafenib may interact with platinum transporter proteins,[17] and exerts a synergistic anticancer effect with cisplatin in preclinical research.[18,19] The combined regimen of sorafenib with cisplatin has been tested in clinical trials in patients with pediatric HCC,[20] gastric cancer,[21–23] lung cancer,[24,25] nasopharyngeal carcinoma,[26] and solid tumors,[27] with favorable outcomes reported. Therefore, the combination of sorafenib with TAI of cisplatin would be expected to have better antitumor efficacy than sorafenib alone in patients with advanced HCC.

In this study, the safety and tolerability of the combination therapy of sorafenib with TAI using cisplatin were investigated in patients with advanced HCC. Although DLTs included grade 4 increased levels of serum AST (level 1), grade 3 gastrointestinal hemorrhage and grade 3 bacteremia (level 1), and grade 3 hypertension (level 1), sorafenib at 800 mg/day combined with cisplatin at 65 mg/m^2/cycle (level 3) was well tolerated. The common drug-related adverse events that were of grade 3 or 4 severity included increased levels of AST (30%), ALT (20%), amylase (30%), and lipase (30%). Liver dysfunctions of grade 3 or higher severity were reported in <1.0% of patients in the SHARP study and in no patients in the Asia-Pacific study. The increase of serum transaminase level seemed to be more severe in this combination regimen than with sorafenib alone. This may have been due to TAI of cisplatin, because the increased levels of AST for grades 3 and 4 have been previously reported to be 32–44% in TAI of cisplatin alone.[10,28]

In this study, administration of sorafenib should have been suspended according to protocol regulations, if grade 2 HFSR was seen. We did not see severe HFSR, but this might lead to a slightly lower dose intensity of sorafenib. Although these severe toxicities were sometimes observed in this study, this regimen was generally manageable, and 800 mg/day sorafenib and 65 mg/m^2/cycle cisplatin were acceptable to be the recommended doses. We plan to carry out a randomized phase II study comparing the combination of sorafenib and TAI using cisplatin to sorafenib alone to evaluate the efficacy and safety of the combination at the recommended doses in patients with advanced HCC.

In conclusion, the combination of sorafenib at 800 mg/day combined with cisplatin at 65 mg/m^2/cycle was determined to be the recommended regimen for a phase II study in patients with advanced HCC. This regimen was generally manageable, and a randomized phase II trial of sorafenib alone versus the

combination of sorafenib with TAI of cisplatin is presently underway.

Acknowledgments

We are grateful to Dr. Junji Furuse, Dr. Keigo Osuga, and Dr. Yasuhiro Matsumura, who served on the efficacy and safety evaluation committee, and to Ms Yoko Yoshimoto, who served on an independent data monitoring committee. We also thank the office administrators (Ms Keiko Kondo and Ms Rubi Mukouyama) for their support. This study was supported by a Grant-in-Aid for Cancer Research from the Ministry of Health, Labour and Welfare, Japan.

Disclosure Statement

Sorafenib (BAY43-9006) was provided without contribution by Bayer Health Care Pharmaceuticals (West Haven, CT, USA), before it was authorized by the Ministry of Health, Labour and Welfare in Japan. Dr. Masafumi Ikeda received lecture fees and research funding from Bayer Yakuhin Ltd, Japan.

Abbreviations

AFP	alpha-fetoprotein
5-FU	5-fluorouracil
ALT	alanine aminotransferase
AST	aspartate aminotransferase
DCP	des-γ-carboxy prothrombin
DLT	dose-limiting toxicity
γ-GT	γ-glutamyl transpeptidase
HCC	hepatocellular carcinoma
HFSR	hand–foot skin reaction
OS	overall survival
PFS	progression-free survival
TACE	transcatheter arterial chemoembolization
TAI	transcatheter arterial infusion
ULN	upper limit of normal

References

1 Jemal A, Bray F, Center MM, Ferlay J, Ward E, Forman D. Global cancer statistics. *CA Cancer J Clin* 2011; **61**: 69–90.
2 Llovet JM, Burroughs A, Bruix J. Hepatocellular carcinoma. *Lancet* 2003; **362**(9399): 1907–17.
3 Llovet JM, Di Bisceglie AM, Bruix J *et al.* Design and endpoints of clinical trials in hepatocellular carcinoma. *J Natl Cancer Inst* 2008; **100**: 698–711.
4 Bruix J, Sherman M. Management of hepatocellular carcinoma: an update. *Hepatology* 2011; **53**: 1020–2.
5 Llovet JM, Ricci S, Mazzaferro V *et al.* Sorafenib in advanced hepatocellular carcinoma. *N Engl J Med* 2008; **359**: 378–90.
6 Cheng AL, Kang YK, Chen Z *et al.* Efficacy and safety of sorafenib in patients in the Asia-Pacific region with advanced hepatocellular carcinoma: a phase III randomised, double-blind, placebo-controlled trial. *Lancet Oncol* 2009; **10**: 25–34.
7 Ensminger WD, Gyves JW. Regional chemotherapy of neoplastic diseases. *Pharmacol Ther* 1983; **21**: 277–93.
8 Tzoracoleftherakis EE, Spiliotis JD, Kyriakopoulou T, Kakkos SK. Intra-arterial versus systemic chemotherapy for non-operable hepatocellular carcinoma. *Hepatogastroenterology* 1999; **46**: 1122–5.
9 Court WS, Order SE, Siegel JA *et al.* Remission and survival following monthly intraarterial cisplatinum in nonresectable hepatoma. *Cancer Invest* 2002; **20**: 613–25.
10 Yoshikawa M, Ono N, Yodono H, Ichida T, Nakamura H. Phase II study of hepatic arterial infusion of a fine-powder formulation of cisplatin for advanced hepatocellular carcinoma. *Hepatol Res* 2008; **38**: 474–83.
11 Okuda K, Tanaka M, Shibata J *et al.* Hepatic arterial infusion chemotherapy with continuous low dose administration of cisplatin and 5-fluorouracil for multiple recurrence of hepatocellular carcinoma after surgical treatment. *Oncol Rep* 1999; **6**: 587–91.
12 Sakon M, Nagano H, Dono K *et al.* Combined intraarterial 5-fluorouracil and subcutaneous interferon-alpha therapy for advanced hepatocellular carcinoma with tumor thrombi in the major portal branches. *Cancer* 2002; **94**: 435–42.
13 Lencioni R, Kudo M, Ye SL *et al.* GIDEON (Global Investigation of therapeutic DEcisions in hepatocellular carcinoma and Of its treatment with sorafeNib): second interim analysis. *Int J Clin Pract* 2013. doi: 10.1111/ijcp.12352. [Epub ahead of print].
14 Furuse J, Ishii H, Nakachi K, Suzuki E, Shimizu S, Nakajima K. Phase I study of sorafenib in Japanese patients with hepatocellular carcinoma. *Cancer Sci* 2008; **99**: 159–65.
15 Abou-Alfa GK, Johnson P, Knox JJ *et al.* Doxorubicin plus sorafenib vs doxorubicin alone in patients with advanced hepatocellular carcinoma: a randomized trial. *JAMA* 2010; **304**: 2154–60.
16 Okada S, Okazaki N, Nose H, Shimada Y, Yoshimori M, Aoki K. A phase 2 study of cisplatin in patients with hepatocellular carcinoma. *Oncology* 1993; **50**(1): 22–6.
17 Heim M, Scharifi M, Zisowsky J *et al.* The Raf kinase inhibitor BAY 43-9006 reduces cellular uptake of platinum compounds and cytotoxicity in human colorectal carcinoma cell lines. *Anticancer Drugs* 2005; **16**: 129–36.
18 Chen FS, Cui YZ, Luo RC, Wu J, Zhang H. Coadministration of sorafenib and cisplatin inhibits proliferation of hepatocellular carcinoma HepG2 cells in vitro. *Nan Fang Yi Ke Da Xue Xue Bao* 2008; **28**: 1684–7.
19 Wei Y, Shen N, Wang Z *et al.* Sorafenib sensitizes hepatocellular carcinoma cell to cisplatin via suppression of Wnt/beta-catenin signaling. *Mol Cell Biochem* 2013; **381**: 139–44.
20 Schmid I, Haberle B, Albert MH *et al.* Sorafenib and cisplatin/doxorubicin (PLADO) in pediatric hepatocellular carcinoma. *Pediatr Blood Cancer* 2012; **58**: 539–44.
21 Sun W, Powell M, O'Dwyer PJ, Catalano P, Ansari RH, Benson AB 3rd. Phase II study of sorafenib in combination with docetaxel and cisplatin in the treatment of metastatic or advanced gastric and gastroesophageal junction adenocarcinoma: ECOG 5203. *J Clin Oncol* 2010; **28**: 2947–51.
22 Kim C, Lee JL, Choi YH *et al.* Phase I dose-finding study of sorafenib in combination with capecitabine and cisplatin as a first-line treatment in patients with advanced gastric cancer. *Invest New Drugs* 2012; **30**: 306–15.
23 Yamada Y, Kiyota N, Fuse N *et al.* A phase I study of sorafenib in combination with S-1 plus cisplatin in patients with advanced gastric cancer. *Gastric Cancer* 2014; **17**: 161–72.
24 Davies JM, Dhruva NS, Walko CM *et al.* A phase I trial of sorafenib combined with cisplatin/etoposide or carboplatin/pemetrexed in refractory solid tumor patients. *Lung Cancer* 2011; **71**: 151–5.
25 Paz-Ares LG, Biesma B, Heigener D *et al.* Phase III, randomized, double-blind, placebo-controlled trial of gemcitabine/cisplatin alone or with sorafenib for the first-line treatment of advanced, nonsquamous non-small-cell lung cancer. *J Clin Oncol* 2012; **30**: 3084–92.
26 Xue C, Huang Y, Huang PY *et al.* Phase II study of sorafenib in combination with cisplatin and 5-fluorouracil to treat recurrent or metastatic nasopharyngeal carcinoma. *Ann Oncol* 2013; **24**: 1055–61.
27 Schultheis B, Kummer G, Zeth M *et al.* Phase IB study of sorafenib in combination with gemcitabine and cisplatin in patients with refractory solid tumors. *Cancer Chemother Pharmacol* 2012; **69**: 333–9.
28 Ikeda M, Okusaka T, Furuse J *et al.* A multi-institutional phase II trial of hepatic arterial infusion chemotherapy with cisplatin for advanced hepatocellular carcinoma with portal vein tumor thrombosis. *Cancer Chemother Pharmacol* 2013; **72**: 463–70.

Laboratory Investigation (2014) 94, 192–207

Cytoglobin is expressed in hepatic stellate cells, but not in myofibroblasts, in normal and fibrotic human liver

Hiroyuki Motoyama[1], Tohru Komiya[2], Le Thi Thanh Thuy[1], Akihiro Tamori[1], Masaru Enomoto[1], Hiroyasu Morikawa[1], Shuji Iwai[1], Sawako Uchida-Kobayashi[1], Hideki Fujii[1], Atsushi Hagihara[1], Etsushi Kawamura[1], Yoshiki Murakami[1], Katsutoshi Yoshizato[1,3] and Norifumi Kawada[1]

Cytoglobin (CYGB) is ubiquitously expressed in the cytoplasm of fibroblastic cells in many organs, including hepatic stellate cells. As yet, there is no specific marker with which to distinguish stellate cells from myofibroblasts in the human liver. To investigate whether CYGB can be utilized to distinguish hepatic stellate cells from myofibroblasts in normal and fibrotic human liver, human liver tissues damaged by infection with hepatitis C virus (HCV) and at different stages of fibrosis were obtained by liver biopsy. Immunohistochemistry was performed on histological sections of liver tissues using antibodies against CYGB, cellular retinol-binding protein-1 (CRBP-1), α-smooth muscle actin (α-SMA), thymocyte differentiation antigen 1 (Thy-1), and fibulin-2 (FBLN2). CYGB- and CRBP-1-positive cells were counted around fibrotic portal tracts in histological sections of the samples. The expression of several of the proteins listed above was examined in cultured mouse stellate cells. Quiescent stellate cells, but not portal myofibroblasts, expressed both CYGB and CRBP-1 in normal livers. In fibrotic and cirrhotic livers, stellate cells expressed both CYGB and α-SMA, whereas myofibroblasts around the portal vein expressed α-SMA, Thy-1, and FBLN2, but not CYGB. Development of the fibrotic stage was positively correlated with increases in Sirius red-stained, α-SMA-positive, and Thy-1-positive areas, whereas the number of CYGB- and CRBP-1-positive cells decreased with fibrosis development. Primary cultured mouse stellate cells expressed cytoplasmic CYGB at day 1, whereas they began to express α-SMA at the cellular margins at day 4. Thy-1 was undetectable throughout the culture period. In human liver tissues, quiescent stellate cells are CYGB positive. When activated, they also become α-SMA positive; however, they are negative for Thy-1 and FBLN2. Thus, CYGB is a useful marker with which to distinguish stellate cells from portal myofibroblasts in the damaged human liver.
Laboratory Investigation (2014) **94,** 192–207; doi:10.1038/labinvest.2013.135; published online 2 December 2013

KEYWORDS: α-smooth muscle actin; cellular retinol binding protein-1; chronic hepatitis; cytoglobin; fibulin-2; Thy-1

Stellate cell activation-associated protein was originally discovered by proteomic analysis (in 2001)[1] in cultured rat hepatic stellate cells that have vitamin A storage ability when quiescent and function as liver-specific pericytes. Histoglobin[2] and Cytoglobin (CYGB)[3] were reported by Trent and Hargrove[2] and by Burmester *et al*,[3] respectively, in 2002. These proteins, in addition to stellate cell activation-associated protein, were classified as human, mouse, and rat homologs of a hexacoordinate globin that differs from the traditional pentacoordinate globins, such as myoglobin and hemoglobin.[4] CYGB consists of 190 amino acids with a calculated molecular mass of 21 kDa, and its amino acid sequence is highly conserved among species.[3] Human CYGB has ~25% amino acid identity with vertebrate myoglobin and hemoglobin and 16% identity with human neuroglobin, which is another type of globin that is present specifically in the nervous system. CYGB is thus recognized as the fourth globin of mammals.[5] The *CYGB* gene is located on human chromosome 17q25.3 and mouse chromosome 11E2.

Although myoglobin, hemoglobin, and neuroglobin are tissue restricted to cardiomyocytes and skeletal myofibers, erythrocytes, and the nervous system, respectively, CYGB is ubiquitously expressed in the cytoplasm of mesenchymal fibroblastic cells of many organs,[6] and CYGB was reported to

[1]Department of Hepatology, Graduate School of Medicine, Osaka City University, Osaka, Japan; [2]Department of Biological Function, Faculty of Science, Osaka City University, Osaka, Japan and [3]PhoenixBio, Higashihiroshima, Hiroshima, Japan
Correspondence: Dr N Kawada, MD, PhD, Department of Hepatology, Graduate School of Medicine, Osaka City University, 1-4-3 Asahimachi, Abeno, Osaka 545-8585, Japan.
E-mail: kawadanori@med.osaka-cu.ac.jp

Received 26 April 2013; revised 20 September 2013; accepted 4 October 2013

be present in the nucleus of human hepatocytes.[7] In particular, CYGB is present in stellate cells in the liver and pancreas, reticulocytes in the spleen, mesenchymal cells in the submucosal layer of the gut, and mesangium cells and stromal cells in the rat kidney. Therefore, one interesting aspect of CYGB expression is its presence in visceral cells that have the ability to store vitamin A. CYGB has also been observed in some neuronal subpopulations of the central and peripheral nervous systems in humans.

Hepatic stellate cells have conventionally been recognized as hepatic fibroblastic cells (myofibroblasts are also categorized as this cell type) that preferentially localize to the portal region. Considering that quiescent stellate cells are transformed into activated stellate cells, the liver contains at least three types of fibroblastic cells: stellate cells, activated stellate cells, and portal myofibroblasts.[8,9] Stellate cells are desmin positive in rodents[10] and, when activated, they express α-smooth muscle actin (α-SMA). In addition, these cells express cellular retinol-binding protein-1 (CRBP-1) and participate in the metabolism of retinol and retinyl esters.[11] In contrast, thymocyte differentiation antigen 1 (Thy-1 or CD90)[12–14] and fibulin-2 (FBLN2)[15–17] have been utilized as markers of liver myofibroblasts. These cell type-specific markers of liver fibroblastic cells have been largely utilized in studies with rodents. However, a specific marker to distinguish stellate cells from myofibroblasts in the human liver has not yet been identified.

The aims of our present work were to investigate whether CYGB is a reliable marker of stellate cells in the normal human liver and to study the expression of CYGB, CRBP-1, Thy-1, FBLN2, and α-SMA in fibrotic and cirrhotic human liver.

MATERIALS AND METHODS

Human Liver Tissues

Human liver tissues damaged by hepatitis C virus (HCV) infection at various fibrosis stages (from F1 to F4, 10 samples each) and one tissue sample damaged by nonalcoholic steatohepatitis (NASH) at fibrosis stage F2 (58-year-old woman with serum alanine aminotransferase (ALT) 110 IU/l) were obtained by liver biopsy at Osaka City University Medical School Hospital (Osaka, Japan) from August 2006 to September 2011. Intact human liver tissues were obtained from patients who had metastatic liver tumors or cholangiocarcinoma treated by surgical resection. The procedures for this study were in accordance with the Helsinki Declaration of 1975 (2000 revision). Liver biopsy was performed after informed consent had been granted.

Clinical Data

The age, sex, and primary clinical data for each patient were obtained on consultation or admission to our university hospital. ALT levels, albumin levels, platelet counts, and anti-HCV antibody levels were measured at the Central Clinical Laboratory of Osaka City University Medical School Hospital (Table 1).

Table 1 Characteristics of the HCV-infected patients enrolled in this study

Stage	Age[a] (years)	ALT[b] (IU/l)	Albumin[a] (g/dl)	Platelet[a] ($\times 10^3$/mm^3)	Grade (A0/A1/A2/A3)
F1	55.5 ± 13.7	63.5 (25.0–89.0)	4.1 ± 0.3	17.9 ± 5.4	3/7/0/0
F2	55.6 ± 8.7	60.2 (40.5–74.0)	3.9 ± 0.3	15.0 ± 5.4	0/5/5/0
F3	63.8 ± 8.1	75.1 (48.2–103.5)	3.8 ± 0.3	12.6 ± 3.2	0/2/5/3
F4	63.0 ± 6.8	82.4 (44.7–115.2)	3.6 ± 0.3	12.0 ± 4.1	0/4/6/0

ALT, alanine aminotransferase.
The stage of liver fibrosis and grade of necroinflammation were assessed based on the new Inuyama classification.[19]
[a]Mean ± s.d.
[b]Median (interquartile range).

Histopathological Diagnosis

Liver biopsy was performed in all 41 patients using a 15-gauge Tru-Cut needle (Hakko, Tokyo, Japan) under ultrasound guidance. The tissue samples fulfilled the size requirements suggested by Janiec *et al*:[18] adequate liver biopsy samples were defined as having a length > 1.0 cm and/or the presence of at least 10 portal tracts. The liver tissues were fixed in 10% formaldehyde, embedded in paraffin, and cut into 4-μm-thick sections. Deparaffinized sections were stained with hematoxylin–eosin and Azan–Mallory, dehydrated in 100% ethanol, cleared by xylene, mounted with NEW M·X (Matsunami Glass Industries, Osaka, Japan), and then examined by microscopy. The degree of liver fibrosis was assessed based on the new Inuyama classification[19] as follows: F0, no fibrosis; F1, expansion of the portal tracts without linkage; F2, portal expansion with portal-to-portal linkage; F3, extensive portal-to-portal and focal portal-to-central linkage; and F4, cirrhosis (Table 1).

The sections were also stained with 0.1% (w/v) Sirius red (Direct Red 80; Aldrich, Milwaukee, WI, USA) in a saturated aqueous picric acid solution for 1 h at room temperature to visualize collagen fibers. After staining, the sections were washed in two changes of 0.01 N HCl and mounted as described above.[20]

Immunostaining of Human Liver Tissues

For immunohistochemistry, paraffin sections were dewaxed in xylene and rehydrated in decreasing concentrations of ethanol (xylene: 3 × 3 min; 100% ethanol: 2 × 3 min; 95% ethanol: 3 min; 70% ethanol: 3 min). Primary antibodies and immunohistochemistry conditions are listed in Table 2. In brief, the sections were deparaffinized and treated with a solution of 3% H_2O_2 in 100% methanol for 10 min at room temperature to block endogenous peroxidase activity.

Table 2 Primary antibodies used in this study

Antibody	Species	Source	Dilution
Anti-human cytoglobin	Rb poly	Our laboratory	1/100
Anti-human cytoglobin	Mo mono	Our laboratory	1/1000
Anti-rat cytoglobin	Rb poly	Our laboratory	1/100
Anti-human cellular retinol-binding protein-1	Rb poly	Santa Cruz	1/100
Anti-human α-smooth muscle actin	Mo mono	Dako	1/100
Anti-human thymocyte differentiation antigen 1 (Thy-1)	Rb poly	Abcam	1/100
Anti-mouse thymocyte differentiation antigen 1 (Thy-1)	Mo mono	Abcam	1/100
Anti-human fibulin-2 (FBLN2)	Rb poly	Sigma	1/200
Anti-human lymphatic vessel endothelial hyaluronan receptor-1 (LYVE-1)	Rb poly	Abcam	1/200

Mo mono, mouse monoclonal antibody; Rb poly, rabbit polyclonal antibody.

The sections were then preincubated with serum-free protein block (Dako, Glostrup, Denmark) for 10 min at room temperature and subsequently incubated with primary antibodies in a dilution of 1:100 for 1 h at room temperature. Negative controls with no primary antibody were used to assess nonspecific staining. The secondary antibodies used included horseradish peroxidase-conjugated goat anti-rabbit IgG (1:200; Dako), rabbit anti-goat IgG (1:200; Dako), and rabbit anti-mouse IgG (1:200; Dako). The chromogen used was 3,3′-diaminobenzidine (Dako). The resultant sections were stained and analyzed using a BZ-8000 microscope (Keyence, Osaka, Japan).

Subsequently, double immunofluorescence staining was performed. After the paraffin sections were dewaxed, the sections were incubated with a mixture of antibodies against CYGB and α-SMA as described previously.[21] After rinsing in PBS, the sections were incubated with a mixture of fluorochrome-conjugated secondary antibodies: AlexaFluor 488 goat anti-rabbit IgG (Molecular Probes, Eugene, OR, USA) and AlexaFluor 594 goat anti-mouse IgG (Molecular Probes). The sections were briefly washed and mounted with ProLong Gold Antifade Reagent (Molecular Probes). The resulting sections were stained and analyzed using a BZ-8000 microscope (Keyence).

Morphometry for Hepatic Fibrosis

For morphometric image analysis of hepatic fibrosis in immunostaining, the areas of the liver sections that were positive for Sirius red (red), α-SMA (brown), or Thy-1 (brown) were captured separately using a charge-coupled device (CCD) camera connected to a macro digital filing system (DP70 · BX-51; Olympus Corporation, Tokyo, Japan). Images representing the whole biopsy section were acquired at × 200 magnification and digitalized. These separately captured and digitalized images were consolidated to create one large image using e-Tiling (Mitani Corporation, Tokyo, Japan). Collagen- or α-SMA-positive areas were measured using Lumina Vision 2.4 (Mitani Corporation) and were calculated automatically. The hepatic fibrotic area (%) was calculated as the area stained with the selected color divided by the whole tissue area at × 100 magnification.[20]

In fibrotic livers, the number of CYGB- and CRBP-1-positive stellate cells in each field was counted around fibrotic portal tracts (F1 to F4 samples). The analysis was performed on each 10-sample group of F1–F4 tissues using an average of five fields per zone (1.4 mm^2) (100 × objective). We counted the cell bodies that stained positively and contained a nucleus.

Cell Lines

The human HSC line LX-2 was donated by Dr Scott L Friedman at the Mount Sinai School of Medicine (New York, NY, USA).[22] LX-2 cells were cultured on plastic dishes or glass chamber slides in Dulbecco's modified Eagle's medium (DMEM; Sigma Chemical, St Louis, MO, USA) supplemented with 10% fetal bovine serum (FBS; Invitrogen, Carlsbad, CA, USA), 100 U/ml penicillin, and 100 μg/ml streptomycin. Huh7 cells (JCRB0403), which were obtained from the Japanese Collection of Research Bioresources (JCRB) Cell Bank (Osaka, Japan), were maintained on plastic culture plates in DMEM supplemented with 10% FBS. In some experiments, LX-2 cells were transfected with the pEGFP-cytoglobin vector (Clontech, Mountain View, CA, USA) using FuGENE HD (Roche, Applied Science, Indianapolis, IN, USA). The cells were collected at 24 h after transfection.

Preparation of Primary Cultured Mouse Hepatic Stellate Cells

Primary mouse stellate cells were isolated from 12- to 16-week-old male C57BL/6N mice (Japan SLC, Shizuoka, Japan) by pronase–collagenase digestion and subsequent purification with a single-step Nycodenz gradient, as previously described.[23] All animals received humane care. The experimental protocol was approved by the Committee

of Laboratory Animals, Osaka City University Medical School, and was performed according to institutional guidelines. Isolated stellate cells were cultured on plastic dishes or glass chamber slides in DMEM (Sigma Chemical) supplemented with 10% FBS (Invitrogen), 100 U/ml penicillin, and 100 μg/ml streptomycin. The purity of the cultures was determined based on observation of the characteristic stellate cell shape using phase-contrast microscopy.

Quantitative Real-Time PCR

Total RNA was extracted from stellate cells using the RNeasy Mini Kit (Qiagen, Valencia, CA, USA). cDNA was synthesized as previously described.[24] Gene expression was measured by quantitative real-time PCR using cDNA, THUNDERBIRD SYBR qPCR Mix Reagents (Toyobo, Osaka, Japan), and a set of gene-specific oligonucleotide primers. The reactions were performed in an Applied Biosystems Prism 7500 Sequence Detection System (Applied Biosystems, Foster City, CA, USA). The expression of glyceraldehyde-3-phosphate dehydrogenase (GAPDH) was also measured as an internal control.

Immunoblotting

Protein samples (30 μg) were subjected to 5–20% gradient SDS-polyacrylamide gel electrophoresis (ATTO, Tokyo, Japan) and transferred to Immobilon P membranes (Millipore Corporation, Bedford, MA, USA). After blocking, the membranes were probed with a primary antibody against CYGB (1:1000; our laboratory), α-SMA (1:2000; Dako), Thy-1 (1:1000; Abcam, Cambridge, UK), or GAPDH (1:2000; Santa Cruz Biotechnology, Santa Cruz, CA, USA). The membranes were then labeled with horseradish peroxidase-conjugated secondary antibodies. Immunoreactive bands were visualized using the ECL detection reagent (GE Healthcare, Buckinghamshire, UK) and documented with an LAS 1000 device (Fuji Photo Film, Kanagawa, Japan).

Data Analysis

The data are presented as bar graphs representing the mean ± s.d. in all experiments. Statistical analyses were performed using Student's *t*-test. $P<0.05$ indicated statistical significance.

RESULTS

Specificity of the Anti-CYGB Antibody

We previously generated rabbit polyclonal anti-rat CYGB antibodies that stain stellate cells in intact and fibrotic rat liver and other visceral organs.[1,25] In the present study, we newly generated rabbit polyclonal and mouse monoclonal antibodies against human CYGB in our laboratory. Immunoblot analysis revealed that the rabbit polyclonal antibodies detected purified recombinant human CYGB,[26] which was provided by RIKEN (Harima, Hyogo, Japan), at 21 kDa and EGFP-binding recombinant human CYGB (generated in our laboratory) at 48 kDa; however, the antibodies did not detect human albumin. LX-2 and Huh 7 cells expressed negligible levels of CYGB (Figure 1a). The monoclonal antibody produced almost identical results (data not shown).

Immunohistochemical Characterization of Intact Human Liver

Intact human liver tissues were obtained by surgical resection from patients with metastatic liver tumors or cholangiocarcinoma, and the expression levels of CYGB, α-SMA, Thy-1, and FBLN2 were determined (Figure 1). As shown in Figure 1bA and B, the obtained tissue samples showed negligible inflammatory cell infiltration and negligible expansion of fibrotic areas. Immunostaining using the polyclonal antibodies against human CYGB revealed positive cells along the sinusoids throughout the lobule (Figure 1bC and D). Similar results were obtained with the monoclonal antibody (Figure 1bE and F). The hepatocytes and the cells in the portal areas were CYGB negative. CYGB-positive cells were present in the serial sections, and we identified these cells as stellate cells because an enlarged view revealed that they were located between the hepatocytes and the lumen of the sinusoids. In addition, these cells contained lipid droplets in their cytoplasm, and their cytoplasmic processes expanded along the sinusoids (Figure 1bD and F).

Immunohistochemistry was further performed on intact human liver samples using antibodies against CRBP-1, α-SMA, FBLN2, and Thy-1. In the liver parenchyma, strong expression of CRBP-1 was observed along the sinusoids (Figure 2a). An enlarged view showed that CRBP-1-positive cells contained lipid droplets, indicating that they were hepatic stellate cells. There were no CRBP-1-positive cells around the portal area. Instead, α-SMA-positive cells predominated; these cells also existed in the walls of the vessels, but not along the hepatic sinusoids (Figure 2b). In addition, the regions adjacent to the portal vein contained limited numbers of cells that stained for FBLN2 or Thy-1 (Figure 2c and d), which are also biomarkers of myofibroblasts.

Taken together, these findings indicate that CYGB and CRBP-1 are uniquely expressed in hepatic stellate cells in the intact human liver, whereas myofibroblast markers such as α-SMA, FBLN2, and Thy-1 are locally present in cells around the portal tract.

Immunohistochemistry of CD68, LYVE-1, and CRBP-1 in Relation to CYGB

CD68 is a glycoprotein that binds to low-density lipoprotein and is expressed by monocytes and macrophages. Kupffer cells are positive for CD68.[27] We found that spindle-shaped CD68-positive cells were present in the sinusoids in the intact human liver, indicating that these cells were Kupffer cells. These cells were predominantly located along the sinusoids (Figure 3a). Double immunofluorescence staining

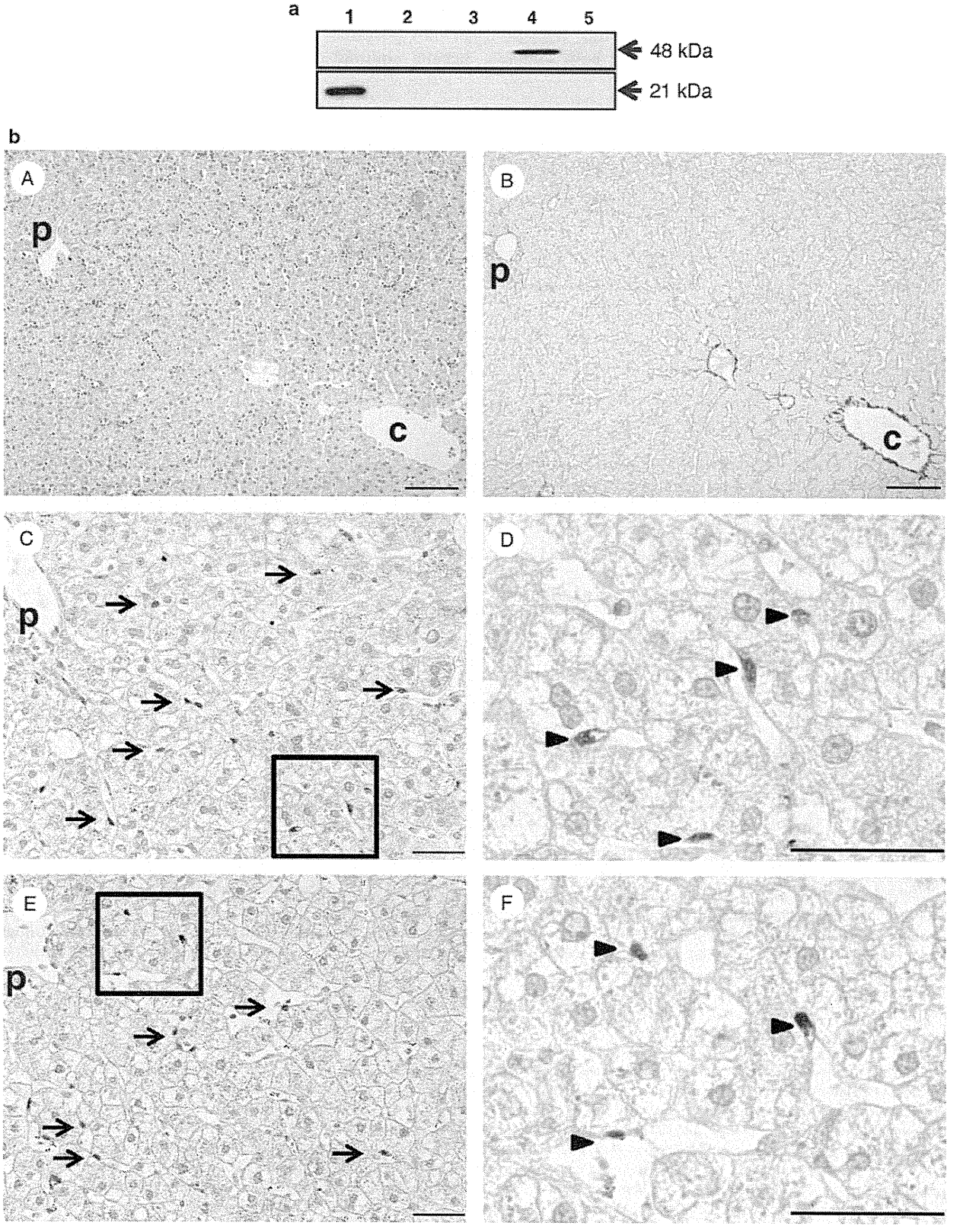
a
1
2
3
4
5
48 kDa
21 kDa
b
A
p
c
B
p
c
C
p
D
E
p
F